THE ASTROPHYSICAL JOURNAL, 314:513–524, 1987 March 15

ON THE ORIGIN OF THE 40–120 MICRON EMISSION OF GALAXY DISKS: A COMPARISON WITH Hα FLUXES

CAROL J. LONSDALE PERSSON AND GEORGE HELOU
Infrared Processing and Analysis Center, California Institute of Technology
Received 1986 May 30; accepted 1986 September 9

ABSTRACT

A comparison of 40–120 μm *IRAS* fluxes with published Hα and *UBV* photometry of galaxy disks shows that the far-infrared emission consists of at least two components: a warm one associated with OB stars in H II regions and young star-forming complexes, and a cooler one from dust in the diffuse, neutral interstellar medium, heated by the more general interstellar radiation field of the disk population (a "cirrus"-like component). Nonionizing stars play a significant role in powering the cool component. The far-infrared (~1–1000 μm) emission of most spiral galaxies is dominated by emission from the cooler component in this model. The model predicts fluxes at $\lambda > 120$ μm in excess of those that would be expected if the 40–120 μm flux were interpreted as a single emission component at the observed temperatures. The available published observations of sample galaxies at $\lambda > 120$ μm (two galaxies) support the model. For blue galaxies with high Hα equivalent width, star-formation rates determined from Hα fluxes are likely to be quite accurate. For most spirals, however, the rates estimated from Hα could be severely underestimated. The far-infrared luminosity is not a very reliable alternative estimator of star-formation rates under normal disk-star forming conditions.

Subject headings: galaxies: photometry — infrared: sources — radiation mechanism

I. INTRODUCTION

With the release of the *IRAS* catalog, fluxes in the 40–120 μm wavelength region have become available for thousands of galaxies. Since the infrared and submillimeter ($\lambda \sim$ 1–1000 μm) flux from normal (nonactive and nonstarburst) spiral and irregular galaxies typically constitutes at least 30% of the total power (Telesco and Harper 1980; de Jong *et al.* 1984; Chini *et al.* 1984*a*, *b*), these data are of fundamental interest for the study of galactic structure, evolution, and stellar populations. The far-infrared flux is often attributed to dust heated by OB stars because in the Galaxy, complexes of such stars embedded in giant molecular clouds (GMC) are the most prominent and efficient sources of far-infrared emission (Becklin, Fomalont, and Neugebauer 1973; Rieke and Lebofsky 1978; Telesco and Harper 1980). Under these physical conditions, the *IRAS*-measured luminosity would be a powerful observational tool, being related to the OB star-formation rate.

The interpretation of the *IRAS*-measured luminosities in terms of a massive star-formation rate is not appropriate for normal disk galaxies. It is really only valid under conditions of high optical depth in and around the H II regions. Much of the *IRAS*-measured far-infrared flux may arise in low-density H II regions, rather than in young, dusty complexes (Mezger 1978; de Muizon and Rouan 1985; Cox, Krugel, and Mezger 1986). The infrared emissivity per Lyman-alpha photon (the so-called infrared excess) in such optically thin conditions is not well known and may vary substantially from galaxy to galaxy, depending on the details of the physical and dynamical environment and the metallicity. Also, disk galaxies emit a substantial fraction of their far-infrared flux at wavelengths greater than the *IRAS* limit of ~120 μm (Telesco and Harper 1980; Smith 1982; Rickard and Harvey 1984; Chini *et al.* 1984*a*, *b*; Thronson *et al.* 1987). Models of the Galactic far-infrared and submillimeter emission indicate that much of this cool emission may arise in the optically thin, neutral interstellar medium, powered to some extent by non-OB stars (Drapatz 1979; de Muizon and Rouan 1985; Cox, Krugel, and Mezger 1986).

In this paper we explore the extent to which the *IRAS*-measured 40–120 μm fluxes of a sample of normal disk galaxies can be attributed to these different regimes (young H II region/GMC complexes, the diffuse neutral medium, and low-density H II regions) and stellar populations (OB stars, A and later stars) by comparison of the 40–120 μm flux with the Hα flux. The sample is taken from Kennicutt and Kent (1983). If the emission of galaxy disks in the *IRAS* bands is dominated by emission from young OB stars (either optically visible or GMC-embedded), the *IRAS* fluxes might be expected to be highly correlated with Hα fluxes. Conversely, a poor correlation of far-infrared with Hα flux might imply a large dispersion in Hα extinction, far-infrared emission from a mixture of H II regions of varying density and dustiness, or a substantial contribution to the far-infrared emission from older and less massive stars. The latter two possibilities would make the *IRAS*-measured far-infrared luminosity less useful as a measure of the star-formation rate.

A future aim, if the *IRAS* data can be unambiguously interpreted, is the reassessment of the OB star-formation rate in galaxy disks. Some star-formation rates determined from the Hα luminosity imply depletion of the gas reservoir in a short period of time (~10^9 yr) (Kennicutt 1983; Gallagher, Hunter, and Tutukov 1984).

The sample and the data are discussed in § II. in § III we present the empirical results. In § IV we argue that both young OB complexes and later type stars contribute to the heating of the dust observed by *IRAS* in galaxy disks. We then present a simple two-component model for the total far-infrared emission. In § V we discuss the consequences of this model.

TABLE 1

OBSERVED AND MODEL-DERIVED PARAMETERS

GALAXY (NGC) (1)	TYPE (RSA) (2)	FLUX DENSITIES (Jy) 12 μm (3)	25 μm (4)	60 μm (5)	100 μm (6)	F_{ir} (W m^{-2}) ($\times 10^{-13}$) (7)	T_c 60/100 (8)	$F_{H\alpha}$ (W m^{-2}) ($\times 10^{-15}$) (9)	IRE (10)	(1.0, 0.1) MODEL IRE$_w^t$ (11)	$F_c^t/(F_c^t + F_w^t)$ (12)	$(F_c^t + F_w^t)/F_{ir}$ (13)
278[a]	Sbc	1.25	2.00	23.4	44.2	13.17	48	14.00	7.9	7.7	0.51	2.0
337	Sc	<0.25	0.62	8.1	16.8	4.74	45	6.24	6.3	5.8	0.57	2.1
450[b]	Sc	<0.11	0.22	2.5	5.0	1.44	46	2.60	4.6	4.3	0.56	2.1
672	SBc	<0.25	0.46	3.3	8.1	2.10	42	5.69	3.1	2.5	0.64	2.3
949[c]	Sc	0.18	0.25	4.2	7.4	2.29	49	3.13	6.1	6.2	0.47	1.9
1084[a]	Sc	1.26	2.30	25.6	54.0	15.11	45	13.60	9.2	8.4	0.57	2.1
1087[a]	Sc	0.61	0.90	9.1	28.8	6.60	37	7.33	7.5	4.8	0.75	2.6
1140	Sb	<0.25	0.43	3.0	4.8	1.57	53	4.12	3.2	3.5	0.40	1.8
1385[a]	Sc	0.78	1.45	15.7	34.7	9.49	44	8.81	9.0	7.9	0.60	2.2
1569[a]	Sm	0.68	6.90	46.3	50.7	21.45	68	51.90	3.5	4.5	0.09	1.4
1637[a]	SBc	0.37	0.98	5.6	13.2	3.50	42	4.32	6.8	5.7	0.63	2.2
1832[a]	SBb	0.36	0.58	6.6	16.6	4.24	41	4.96	7.1	5.7	0.66	2.3
2139[a]	SBc	0.33	0.63	6.6	13.6	3.84	45	5.96	5.4	4.9	0.56	2.1
2276[a]	Sc	0.59	1.14	11.6	28.7	7.39	41	6.68	9.2	7.4	0.65	2.3
2763[c]	Sc	0.16	0.18	2.2	6.2	1.49	39	2.54	4.9	3.5	0.71	2.5
2976[a]	Sd	0.46	0.77	10.1	28.9	6.93	39	11.10	5.2	3.7	0.71	2.5
3351[a]	SBb	0.62	1.93	17.1	34.5	9.91	46	9.44	8.7	8.2	0.55	2.1
3363[a]	Sab	0.45	<0.56	9.0	26.7	6.29	38	5.69	9.2	6.3	0.73	2.5
3389[c]	Sc	0.22	0.40	3.8	9.6	2.46	41	3.43	6.0	4.8	0.66	2.3
4027[a]	Sc	0.54	0.96	10.2	27.3	6.74	40	6.84	8.2	6.1	0.67	2.4
4189[c]	SBc	0.24	0.28	3.2	8.7	2.15	40	2.07	8.7	6.5	0.69	2.4
4212[a]	Sc	<0.41	0.65	6.6	16.1	4.17	42	4.12	8.4	6.8	0.65	2.3
4294[b]	SBc	<0.11	<0.16	2.7	5.5	1.58	46	4.03	3.3	3.0	0.56	2.1
4299[b]	Sd	<0.11	<0.16	2.5	4.8	1.42	48	4.03	2.9	2.9	0.51	2.0
4420[c]	Sc	0.16	0.20	2.6	7.3	1.76	39	3.13	4.7	3.3	0.71	2.5
4449[d]	Sm	1.63	3.95	32.0	66.2	18.75	45	53.10	2.9	2.7	0.56	2.1
4496	SBc	<0.25	<0.77	3.5	9.6	2.36	39	4.22	4.7	3.4	0.69	2.4
4536	Sc	1.42	3.49	30.0	44.0	15.31	55	6.84	18.7	21.2	0.34	1.7
4632[a]	Sc	<0.37	<0.35	3.9	10.5	2.60	40	4.12	5.3	4.0	0.69	2.4
4654[a]	SBa	0.86	1.32	13.0	34.4	8.55	40	5.82	12.2	9.3	0.68	2.4
4689[b]	Sc	0.23	0.26	2.7	9.7	2.08	35	2.92	5.9	3.3	0.80	2.7
4736[d]	Sab	5.33	7.81	64.4	136.0	38.07	45	29.20	10.9	9.9	0.56	2.1
4775[c]	Sc	<0.12	<0.19	3.6	10.3	2.47	39	4.32	4.8	3.4	0.71	2.4
4781[c]	Sc	0.5	0.53	7.4	17.6	4.64	42	4.73	8.2	6.8	0.63	2.3
4790[c]	Sd	<0.12	0.19	2.7	6.1	1.63	43	2.21	6.1	5.2	0.62	2.2
4808	Sc	0.68	0.70	6.7	14.7	4.03	44	4.73	7.1	6.2	0.59	2.2
4900	Sc	0.34	0.47	5.4	11.9	3.25	44	6.24	4.3	3.8	0.59	2.2
5248[a]	Sbc	0.96	1.50	17.5	43.0	11.10	41	9.66	9.6	7.7	0.66	2.3
5633	Sbc	<0.27	0.33	2.7	7.5	1.81	39	1.88	8.0	5.7	0.71	2.5
5676[a]	Sc	0.6	0.92	10.2	29.8	7.07	38	4.96	11.9	8.2	0.72	2.5
5806	Sb	<0.25	<0.44	2.6	8.0	1.86	38	2.26	6.8	4.6	0.73	2.5
5962[a]	Sc	0.59	0.86	8.5	21.4	5.44	41	4.12	11.0	8.7	0.66	2.3
5970	SBbc	<0.34	0.34	2.6	9.2	2.02	35	3.43	4.9	2.8	0.78	2.7
6181	Sa	0.51	1.04	8.8	19.9	5.35	43	5.07	8.8	7.6	0.61	2.2
6207[a]	Sc	<0.25	0.40	4.4	11.3	2.84	41	5.43	4.4	3.4	0.67	2.3
6217[a]	SBbc	0.5	1.55	10.4	20.5	5.95	46	5.31	9.3	8.8	0.54	2.1
6574	Sbc	0.93	1.69	14.3	27.2	8.06	47	3.27	20.5	20.0	0.52	2.0
7137[c]	Sc	0.23	0.31	3.2	7.4	1.98	43	2.11	7.8	6.6	0.62	2.2
7218[c]	Sc	0.23	0.33	4.7	9.8	2.78	45	3.06	7.6	7.0	0.56	2.1
7392[b]	Sbc	0.11	0.23	2.3	7.3	1.66	36	1.60	8.6	5.4	0.76	2.6
7443	Sc	0.41	0.61	7.6	17.6	4.69	43	5.43	7.2	6.1	0.62	2.2
7723	SBb	<0.38	0.53	4.1	10.4	2.65	41	2.16	10.2	8.0	0.66	2.3
IC 4662	Im	<0.25	1.05	8.1	11.4	4.07	57	20.80	1.6	1.9	0.30	1.7
IC 5271[c]	Sb	0.21	0.25	2.9	9.8	2.19	36	0.70	25.9	15.5	0.77	2.6

NOTES.—Cols. (1)–(6): Galaxy identifications and *IRAS* flux densities as given in the Point Source Catalog, unless noted otherwise: [a] The 12 and 25 μm sources are probably extended, rendering the fluxes unrealiable; [b] the 12 and 25 μm fluxes are from co-added survey data; [c] from co-added survey data; [d] from *IRAS* additional observations (Rice 1986).

Col. (7): 40–120 μm flux, as defined in eq. 1.

Col. (8): 60/100 μm color temperature (photometric uncertainty ~3 K).

Col. (9): The Hα flux, corrected for extinction and [N II] emission as explained in the text.

Col. (10): Infrared excess, derived from the data in cols. (7) and (9).

Col. (11): Total IRE of the warm component of the model.

Col. (12): Fraction of the total model far-infrared flux emitted by the cool component.

Col. (13): Ratio of the total model flux to the observed 40–120 μm flux.

II. THE SAMPLE AND THE DATA

a) *The Sample*

Kennicutt and Kent (hereafter KK) (1983) made large-aperture Hα + [N II] observations of over 100 disk galaxies. We have restricted KK's sample to that subset with "high quality" Hα + [N II] fluxes for which all the flux was contained within their largest diaphragm and, with two exceptions, to galaxies that are point sources to *IRAS* at 60 and 100 μm. Galaxies were judged to be point sources if their point-source correlation coefficients were high and they were not associated with small extended sources (*IRAS Explanatory Supplement* 1985; *IRAS Small Scale Structures Catalog* 1986). The exceptions are the galaxies NGC 4449 and NGC 4736 for which high-quality integrated *IRAS* fluxes are available (Rice 1986). We have also required that the 60 μm flux density be greater than 2 Jy, which is 3 times the completeness limit (*IRAS Explanatory Supplement* 1985). Finally, galaxies for which a significant part (>20%, as defined by KK) of the Hα emission originates in the nucleus were excluded since the primary interest here is disk emission. We assume that the far-infrared flux of the resulting sample will be dominated by disk emission, though it is not possible to guarantee this. The resulting sample consists of 54 galaxies, which are listed in Table 1.

b) Hα *Fluxes*

The Hα fluxes, $F_{H\alpha}$, tabulated in column (9) of Table 1, have been corrected for extinction and [N II] emission as recommended by Kennicutt (1983, hereafter K83) and KK. This involves a mean extinction of 1.1 mag at Hα (derived by KK from the limited thermal radio fluxes available) for each galaxy. This correction must be considered uncertain at the 50% level (K83). An average correction for [N II] emission of 75% for spirals and 95% for irregulars (morphological types from Sandage and Tammann 1981; hereafter the RSA) has been applied (K83). This correction introduces 5%–20% uncertainties in the derived Hα fluxes (KK). The photometric uncertainties are less than 10% (KK).

c) *Far-Infrared Fluxes*

i) *Observed 40–120 μm Fluxes*

For the *IRAS* 60 and 100 μm data we have used measurements from the *IRAS Point Source Catalog* (1985), (columns [5] and [6] of Table 1), except for the two extended galaxies noted above and for a few cases in which survey data were reprocessed (see Table 1). All the galaxies surveyed by *IRAS* and detected in Hα by KK with high-quality fluxes were detected at both 60 and 100 μm by *IRAS*. The far-infrared flux in Table 1, column (7), is defined as follows:

$$F_{ir} = 1.26(2.58 \times 10^{12} f_{60} + 1.00 \times 10^{12} f_{100}) 10^{-26} \text{W m}^{-2} \quad (1)$$

(*Cataloged Galaxies and Quasars Observed in the IRAS Survey*, 1985, Appendix B), where f_{60} and f_{100} are the *IRAS* cataloged flux densities in Jy. The multiplicative factors within the parentheses have units of Hz and are the factors required to convert the quoted flux densities back to the measured in-band fluxes (*IRAS Explanatory Supplement* 1985). The factor of 1.26 accounts for the conversion from these bandpasses to a single ideal (square) bandpass with $\lambda_{eff} = 82.5$ μm and $\Delta\lambda = 80$ μm. F_{ir} is essentially independent of the intrinsic energy distribution for typical galaxies (*Cataloged Galaxies and Quasars Observed in the IRAS Survey*). We have chosen not to extrapolate F_{ir} to "total" (~1–1000 μm) far-infrared/submillimeter fluxes for the general analysis because of the uncertainties in the dust grain emissivity law and temperature distribution. It should be noted, therefore, that F_{ir} is an underestimate of the total far-infrared flux, by factors up to ~2 (*Cataloged Galaxies and Quasars Observed in the IRAS Survey*).

The expected photometric uncertainties in the 60 and 100 μm *IRAS* fluxes are ~10%–15% (*IRAS Explanatory Supplement*, chaps. 6 and 7). Some of our sample may be marginally extended at 60 μm, leading to an additional uncertainty of less than 20%.

ii) *Emission at λ < 40 μm*

Emission in the 12 and 25 μm bands was detected form many of the galaxies in the sample (columns [3] and [4] of Table 1), but the fluxes are low, and, unlike at 60 and 100 μm, the 12 and 25 μm emission is often extended compared to the smaller *IRAS* 12 and 25 μm diaphragm, so the fluxes are not well-determined in the *IRAS Point Source Catalog* (1985).

In order to assess how much luminosity is missed at $\lambda < 40$ μm by F_{ir}, we have co-added the *IRAS* survey data for some of the program galaxies that are unresolved at 12 and 25 μm, as noted in Table 1. The 12–100 μm spectral energy distributions are broad and can be fitted with two modified blackbodies with temperatures of 200–300 K and 30–60 K such that only 15%–28% (median 20%) of the total 1–1000 μm flux originates in the warmer component, which emits principally at $\lambda < 40$ μm.

III. RESULTS

The relationship between F_{ir} and $F_{H\alpha}$ is plotted in Figure 1*a*. The correlation between the two quantities appears to be very good, with a slope consistent with unity and a Spearman's rank-order correlation coefficient, $r_S = 0.81$. Figure 1*b*, however, shows just as good a correlation ($r_S = 0.79$) between F_{ir} and the flux within the blue filter, F_{blue} (derived from $B_T{}^0$ from de Vaucouleurs, de Vaucouleurs, and Corwin 1976, hereafter RC2).

It is necessary to check whether either of the relationships evident in Figure 1 are artificially enhanced by an underlying fundamental correlation of each parameter with galaxy mass, or to a distance-dependent selection effect. Since the far-infrared flux may depend on disk (stellar or interstellar) mass, the data are replotted in Figure 2 after normalizing each axis by the square of the angular diameter (D_0 from RC2). Good correlations still exist in this figure ($r_S = 0.87$ and 0.81, respectively). Excellent correlations are also seen when luminosities are plotted instead of fluxes (not shown).

To investigate further the contribution to the far-infrared flux by the stellar population responsible for the blue light, we derive the infrared excess, IRE, defined as the ratio of the infrared luminosity to the Lyman-alpha luminosity: IRE = $L_{ir}/N_c' h\nu_{Ly\alpha}$[1], where N_c' is the number of Lyman continuum photons absorbed by the gas and $h\nu_{Ly\alpha}$ is the energy of a Lyman-alpha photon. This relation assumes that $N_c' \sim N_c = N_{H\alpha}$.

[1] Here, N_c' is derived from the extinction corrected Hα flux using the relation $N_c' = 9.22 \times 10^{12} D^2 F_{H\alpha}$ (D is the distance in cm, and $F_{H\alpha}$ is in ergs^{-1} cm^{-2}; Osterbrock 1974).

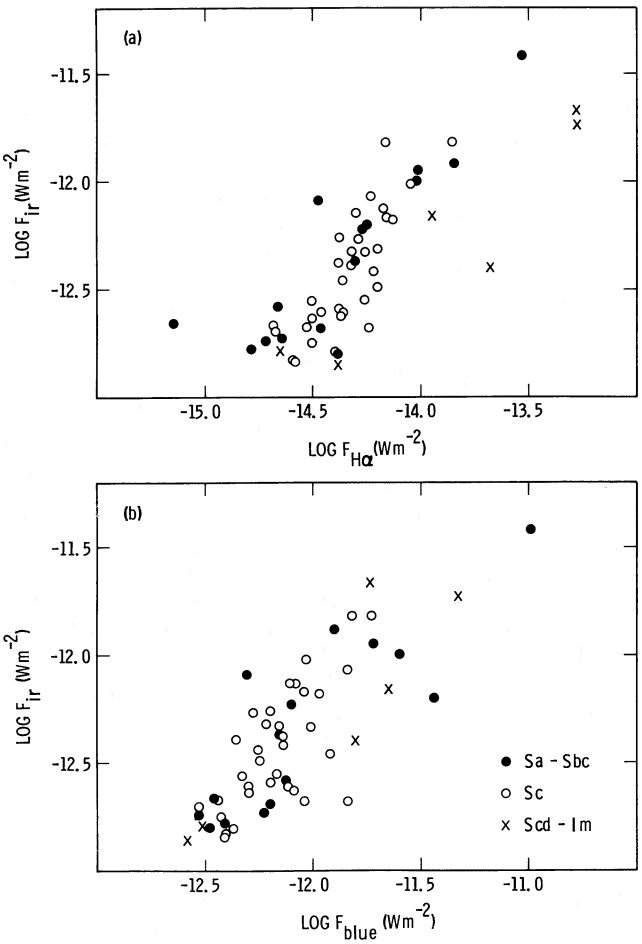

FIG. 1.—Correlation between far-infrared and (*a*) Hα and (*b*) blue fluxes (derived from B_T^0 from de Vaucouleurs, de Vaucouleurs, and Corwin 1976). The 54 galaxies are binned by revised Hubble type (Sandage and Tammann 1981). The far-infrared flux correlates as well with the blue flux as it does with the Hα flux.

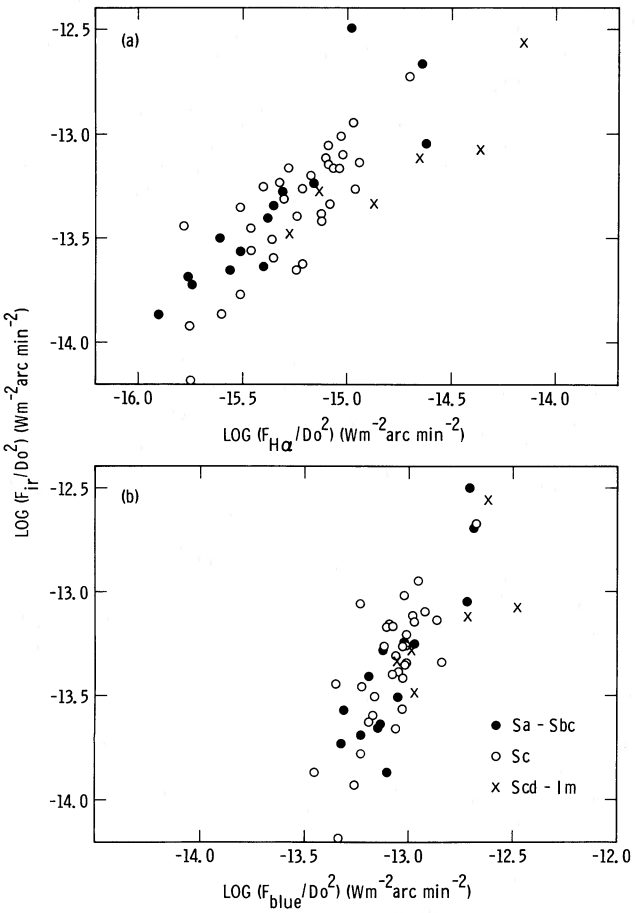

FIG. 2.—The data of Fig. 1 normalized by the square of the corrected blue diameter (from de Vaucouleurs, de Vaucouleurs, and Corwin 1976). The correlations seen here are as good as in Fig. 1, implying that neither distance-dependent selection effects nor a simple scaling with galaxy mass are responsible for the apparent correlations of Fig. 1.

In Figures 3–6 we show the relationships of IRE and the 60/100 μm color temperature, T_c, with the equivalent width of Hα, W_λ(Hα), optical color, and morphological type. IRE is proportional to the ratio of the axes of Figure 1*a*, thus it is a measure of the residuals from the mean relation in that figure. The IRE and T_c are tabulated in Table 1, Columns (8) and (10). W_λ(Hα), derived from the extinction and [N II]-corrected Hα flux as listed in column (9) of Table 1, has been taken from K82.

Figure 3 shows that there is a possible weak negative dependence of IRE on T_c. Figure 4 illustrates that there may be a tendency for IRE to decrease, and T_c to increase with W_λ(Hα), which is a measure of the current relative star-formation rate (K83). Figure 5 shows that galaxies which are red in $(B-V)_T^0$ (fully corrected to face-on from RC2) tend to be cooler in the far-infrared, and to have larger IRE. Similar relationships are seen with $(U-B)_T^0$. In Figure 6, it can be seen that IRE decreases toward later type, as is also clearly visible in Figures 1*a* and 2*a*. W_λ(Hα) increases toward later type, as discussed by K83. While a couple of the very late types are clearly hotter than the rest, no gradient in T_c can be distinguished with type.

Since some trends with observed color temperature are reported here it is important to check whether they are due to

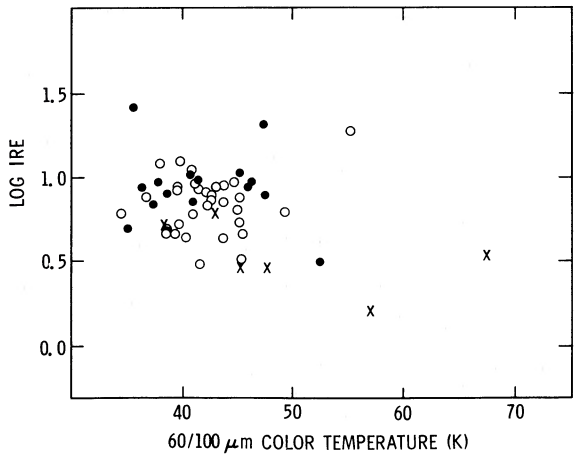

FIG. 3.—The infrared excess vs. far-infrared color temperature. IRE is defined as the 40–120 μm flux in units of the Lyman-alpha flux. There is a slight tendency for IRE to decrease with temperature.

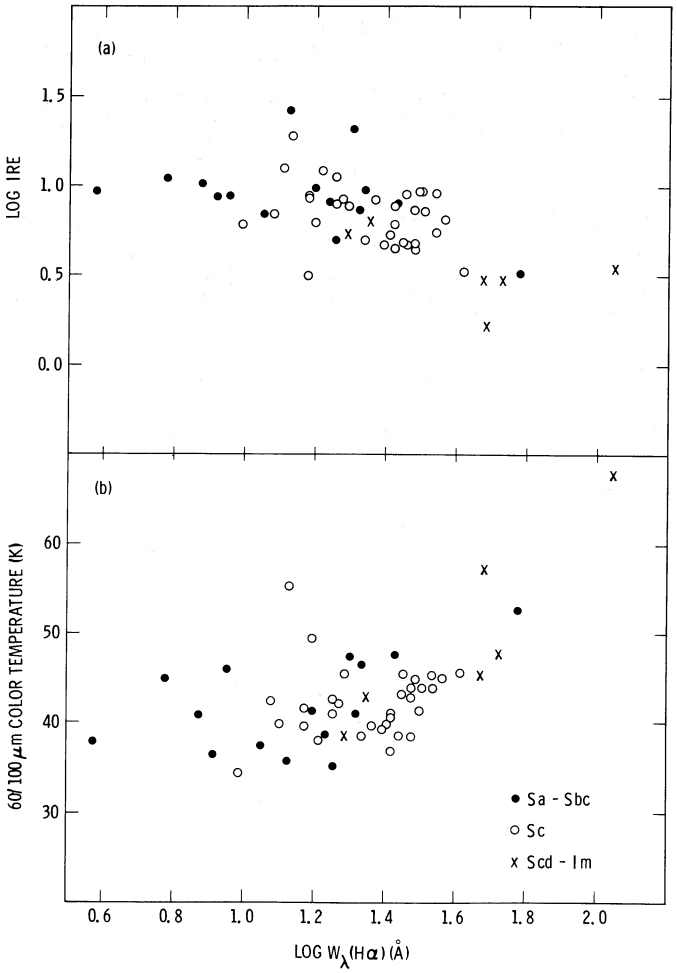

FIG. 4.—Relationships between the equivalent width of Hα and (*a*) the infrared excess (the 40–120 μm flux in units of the Lyman-alpha flux) and (*b*) the 60/100 μm color temperature. IRE appears to decrease with W_λ while the color temperature may increase with W_λ.

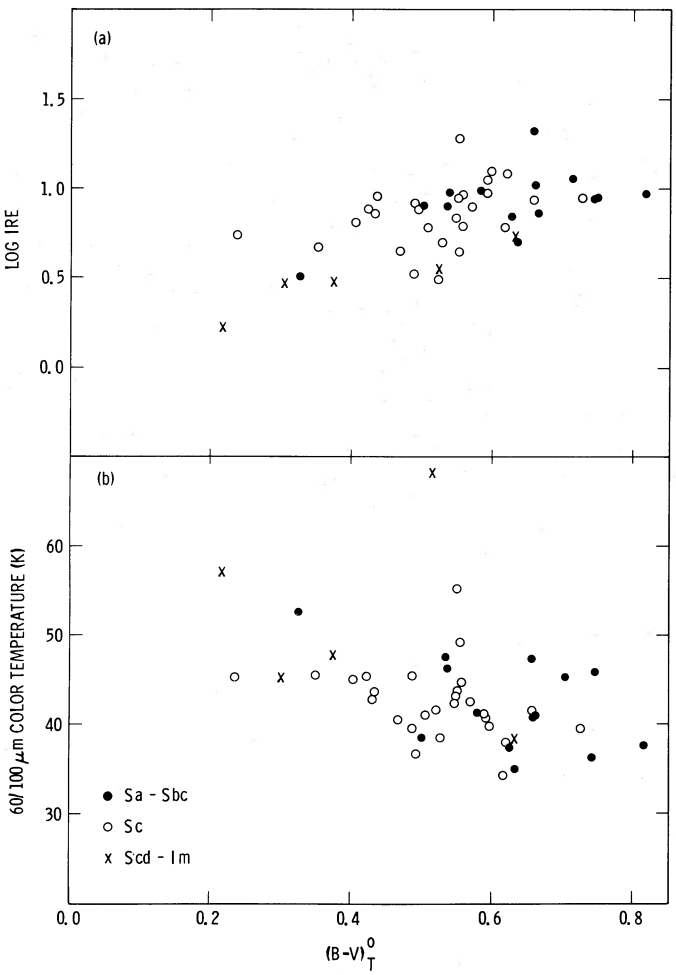

FIG. 5.—Relationships between $(B-V)_T^0$ (from de Vaucouleurs, de Vaucouleurs, and Corwin 1976) and (*a*) the infrared excess and (*b*) 60/100 μm color temperature. Redder galaxies appear to be cooler in the far-infrared and to have larger infrared excess.

the fact that the fraction of the total far-infrared flux intercepted by the 60 and 100 μm bands depends on the dust temperature. In fact the range in observed 60/100 μm color temperature is small enough that the character of Figures 1–6 remains unchanged when the "total" far-infrared flux (obtained by integrating under a modified Planck curve of the form $f_\nu \propto \nu^n B[\nu, T]$) is plotted instead of F_{ir}.

IV. INTERPRETATION AND MODELING

On the basis of Figures 1 and 2 we conclude that the 40–120 μm flux of galaxies may be powered in part by the stellar populations responsible for the blue flux, in addition to the H II regions. The blue flux is dominated by old disk stars with a characteristic mass 1–2 $M_\odot$ (Searle, Sargent, and Bagnuolo 1973; Lequeux 1986; Renzini and Buzzoni 1986), which implies significant input to the far-infrared flux from non-OB stars.

Figures 3-6 show some additional weak trends in the data such that the coolest galaxies, which have 60/100 μm ratios similar to that of Galactic cirrus emission (Gautier 1986), tend to have high IRE, low W_λ(Hα), and red *UBV* colors. At the warm end of the T_c distribution, the 60/100 μm values are more typical of compact H II regions (Chini *et al.* 1986*a*, *b*). For these objects, IRE tends to be low, W_λ(Hα) high, and the *UBV* colors blue. Thus a picture emerges in which high IRE is apparently anticorrelated with optical indicators of a high star-formation rate (high W_λ[Hα] and blue *UBV* color) and with dust temperature.

Three ways to explain the apparent anticorrelation of IRE with optical star-formation rate indicators might be invoked. (1) The simplest possibility is that the far-infrared flux is powered predominantly by OB stars. The trends seen in Figures 3–6 would then be due to a large dispersion in dust optical depth such that low W_λ(Hα) and red *UBV* colors are due to extinction and reddening rather than to low star-formation rate. The corresponding high IRE would be due both to a depression of the Hα flux and to an enhancement of the fraction of primary photons absorbed by dust and reradiated in the far-infrared. A strong objection to this model is that if the decrease in $B-V$ in Figure 5*a* were to be attributed to reddening, an A_v of more than two would be required. This is much larger than typical galaxian internal extinctions (RC2). Also, there is a rough separation by Hubble type in Figure 5 in a sense consistent with dominance of the $B-V$ color by stellar populations rather than by reddening.

(2) If the *UBV* colors are a true reflection of the stellar population, a natural interpretation of Figures 1–6 is that there

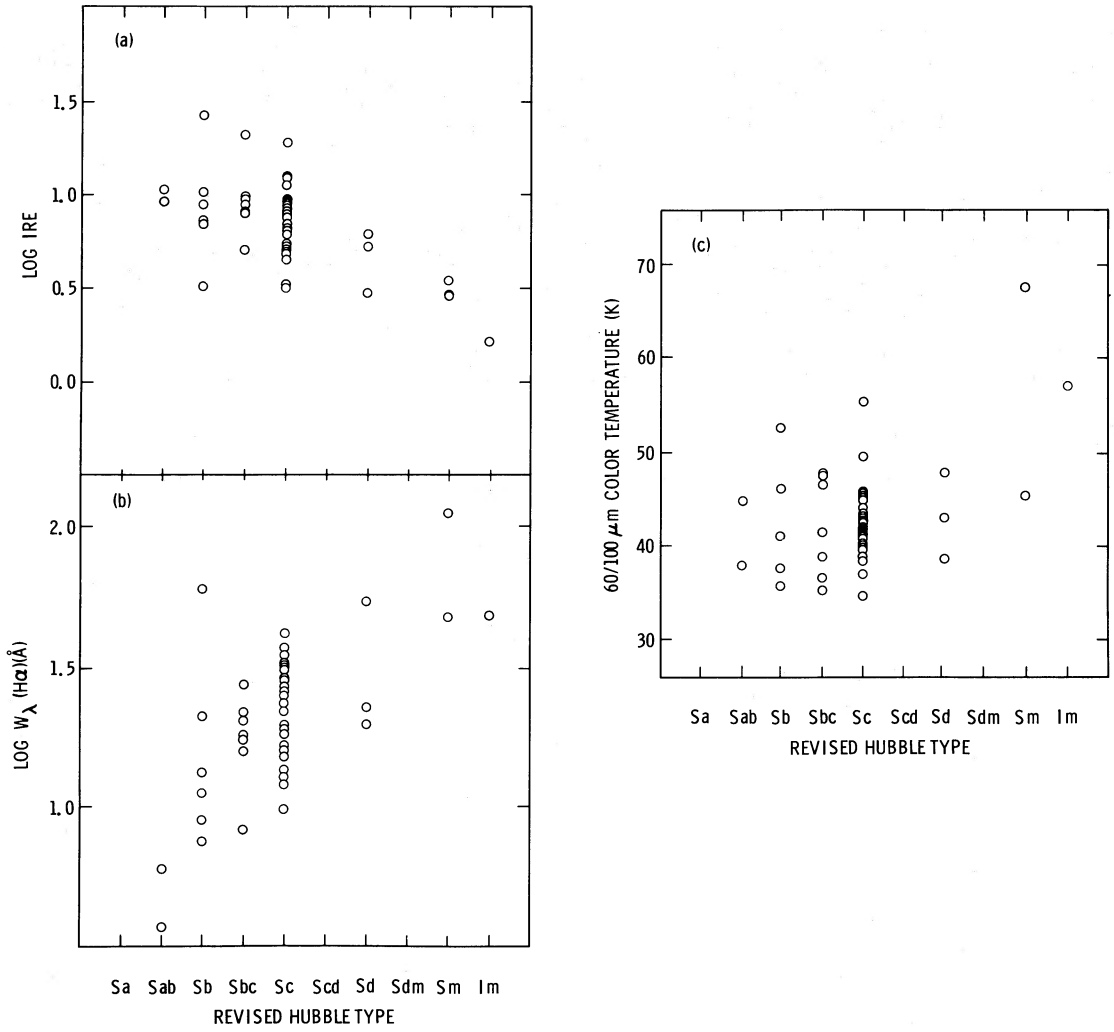

FIG. 6.—Distributions of (*a*) infrared excess, (*b*) equivalent width of Hα and (*c*) 60/100 μm color temperature with revised Hubble type (from Sandage and Tammann 1981).

are at least two far-infrared flux components contributing to the *IRAS*-observed emission: a warm, low-IRE one originating with the OB star population and a cooler high-IRE one powered by the general interstellar radiation field and not strongly related to the H II regions. This is similar in concept to the models for the far-infrared emission of the Galaxy proposed by de Muizon and Rouan (1985) and Cox, Krugel, and Mezger (1986) and to the models proposed for other galaxies by Rowan-Robinson and Crawford (1986), de Jong (1986), and Helou (1986*b*). The warm component would dominate in the bluer, high star-formation rate galaxies and the cooler one in the redder, low star-formation rate galaxies.

(3) A third possibility is that the variations in observed IRE are driven by a changing IMF, such that the H II regions in the high W_λ(Hα) galaxies are powered by hotter stars than in the lower W_λ(Hα) galaxies, leading to higher dust temperatures and lower IREs (Panagia 1974). This effect is likely to be operating to some extent in the high star-formation rate, late-type galaxies such as NGC 4449 and NGC 1569. It is somewhat artificial for large disks undergoing steady-state star formation.

We favor the second possibility described above as the most likely scenario for spiral disks with steady-state star formation, which make up the bulk of our sample. Besides the objections raised to the other models, we favor the second interpretation because (*a*) there exist normal H I-rich spirals with little or no detectable Hα flux, which are not particularly dusty yet have normal *IRAS*-measured far-infrared fluxes (Bothun 1986); (*b*) interstellar radiation field-heated dust that is associated with neutral material is known to exist in the Galaxy (the "cirrus" of Low *et al.* 1984; Gautier 1986), and $\lambda > 100$ μm observations of galaxies imply the existence of a fairly cool (~ 20 K) dust emission component there too (Telesco and Harper 1980; Smith 1982; Rickard and Harvey 1984; Chini *et al.* 1984*a*, *b*; Thronson *et al.* 1987); (*c*) as noted above, this scenario is consistent with detailed models of the far-infrared diffuse emission of our own Galaxy (de Muizon and Rouan 1985; Cox, Krugel, and Mezger 1986); and (*d*) there is evidence that the scale height of the Galactic 100 μm diffuse emission is considerably larger than that of the molecular layer (Burton *et al.* 1986; Perault *et al.* 1986). We therefore consider a two-component model for the spirals in our sample. We apply this model to the very late-type galaxies as well but expect that the effects of a variable IMF (scenario no. 3 above) may also be relevant to them.

a) The Model

We define the two components of our model as follows: a "warm" component associated with the young OB star population and a "cool" one associated with interstellar radiation field heating of diffuse neutral material. All the Hα flux is associated with the warm component. The main simplifying assumptions are that there are only two dust emission components with single-valued dust temperatures, and that these components are the same for all galaxies. The available data cannot constrain a more complex model. In reality, there is not likely to be a sharp boundary in either space or temperature. The model also assumes implicitly that the H II region luminosity function is similar from galaxy to galaxy, since it deals with a single warm emission component of given far-infrared and Hα flux, whereas the warm far-infrared emission may come preferentially from the denser, dustier H II regions while the Hα flux is dominated by the larger, more evolved low-density H II regions (Kennicutt 1984).

Each model is defined by the 60/100 μm flux density ratio of the warm (denoted by "w") and cool (denoted by "c") component, and is therefore hereafter referred to in the notation ($60/100_w$, $60/100_c$). These model ratios must clearly lie at or beyond the extrema of the observed distribution of 60/100 μm flux density ratio. They were chosen with this in mind and also to be consistent with colors of cirrus (Gautier 1986) and of H II complexes (Chini *et al.* 1986*a*, *b*). The ratios considered and their corresponding dust temperatures for various values of dust emissivity law index, n (defined such that the flux density $f_\nu \propto \nu^n B[\nu, T]$), are listed in Table 2. For each galaxy and each model the combination of the two components was found that matches the observed F_{ir} and 60/100 μm ratio. This fixes the absolute 40–120 μm fluxes of the two components, F_w and F_c. "Total" far-infrared fluxes, F_w^t and F_c^t, have also been derived by integrating a modified Planck spectrum of the form $\nu^n B[\nu, T]$, adopting a dust emissivity law index, n, of 2 (see Appendix), and where T is defined by the observed 60/100 μm ratio and n[2]. Since it is assumed that the Hα flux is associated with the warm component only, IREs for this component alone are derived, $\mathrm{IRE}_w = F_w/F_{\mathrm{Ly}\alpha}$, and $\mathrm{IRE}_w{}^t = F_w{}^t/F_{\mathrm{Ly}\alpha}$.

[2] When referring to "total" fluxes derived in this manner, we retain the quotation marks to remind the reader that these fluxes are estimates, based on a single temperature extrapolation, not true observed total fluxes.

TABLE 2

MODEL DUST TEMPERATURES

(60/100) RATIO (1)	T_d $n = 0$ (2)	$n = 1$ (3)	$n = 2$ (4)	N (5)
0.5, 0.1	45, 23	36, 20	30, 18	45
0.5, 0.2	45, 30	36, 26	30, 22	45
0.5, 0.3	45, 35	36, 30	30, 26	42
1.0, 0.1	70, 23	51, 20	40, 18	54
1.0, 0.2	70, 30	51, 26	40, 22	54
1.0, 0.3	70, 35	51, 30	40, 26	51
2.0, 0.1	150, 23	80, 20	56, 18	54
2.0, 0.2	150, 30	80, 26	56, 22	54
2.0, 0.3	150, 35	80, 30	56, 26	51

Cols. (1)–(4): 60/100 μm flux density ratio, and dust temperatures for various choice of n, for each model considered. The parameters are paired, the warm model component being given first, then the cool. Col. (5): number of galaxies fitted by the model.

b) Model Viability

A fundamental test for the model is that F_w should correlate better with $F_{\mathrm{H}\alpha}$ than with F_{blue}, and F_c should correlate better with F_{blue} than with $F_{\mathrm{H}\alpha}$. We have examined these correlations for each model listed in Table 2. There is a general trend such that Spearman's rank-order correlation coefficient for the relation between F_w and $F_{\mathrm{H}\alpha}$ is higher than for the relation between F_c and $F_{\mathrm{H}\alpha}$. Likewise, F_c tends to correlate better with F_{blue} than does F_w. However, the differences between the correlation coefficients are not usually significant at the 98% level. This lack of clear improvement is very likely to be due to the over-simplified nature of the model.

No one model was found to be clearly better than any other when the test described above was made. We interpret this to mean that the *IRAS* data are not very sensitive to the temperature of the cool dust emission. We do find that the five models with either $(60/100_w) = 0.5$ or $(60/100_c) = 0.3$ or both cannot fit all galaxies and generally produce poorer correlations. In what follows we adopt one of the remaining four, the (1.0, 0.1) model, as a specific example, since its dust temperatures reflect those of active star-forming regions and cirrus well. We refer to all four models that are capable of fitting all galaxies as the "preferred models."

A requirement of the model is that it must not predict 12 and 25 μm fluxes that exceed the observed fluxes. For some choices of dust temperature the model prediction matches or slightly exceeds the observed 25 μm flux density, but not by a significant amount. At 12 μm the model always predicts flux densities much smaller than observed, so clearly another emission component operates here. We return to this point briefly in § V*c*.

c) Model Results

The distribution of the fraction of the "total" far-infrared flux arising in the cool component, $F_c{}^t/(F_c{}^t + F_w{}^t)$ is shown in Figure 7, and also tabulated for the (1.0, 0.1) model in Table 1 (column [12]). The cool component has somewhat more flux than the warm for most galaxies for the preferred models. The ratio $F_w{}^t/F_c{}^t$ is sensitive to the choice of $60/100_w$ and $60/100_c$, and hence is not well determined for any particular galaxy.

The ratio of the "total" model flux to the observed 40–120 μm flux, $(F_c^t + F_w^t)/F_{ir}$, is typically 2–2.5 for the preferred models (column [13] of Table 1). The "total" model far-infrared flux is larger than "total" fluxes derived under the assumption that the far-infrared emission can be characterized by a single-component modified Planck spectrum, at the observed 60/100 μm color temperature, by factors of 1.5–2.

The "total" IRE of the warm component, $IRE_w{}^t$, is given in Table 1 (column [11]) and its distribution for all models is illustrated in Figure 8; it lies in the range 2–10 for the bulk of the sample for $n = 2$. Three galaxies with abnormally large IREs, NGC 4536, NGC 6574, and IC 5271, may be dominated by active or starburst nuclei.

V. DISCUSSION

We have shown that the *IRAS*-measured far-infrared flux of galaxy disks is not likely to be powered solely by young OB stars but also has a contribution from the older population seen in the blue. The results of a simple two-component model based on this interpretation are that for most galaxies a cool component, interpreted as "cirrus" emission (dust in the diffuse neutral interstellar medium heated by the interstellar radiation field), is responsible for more than 50% of the

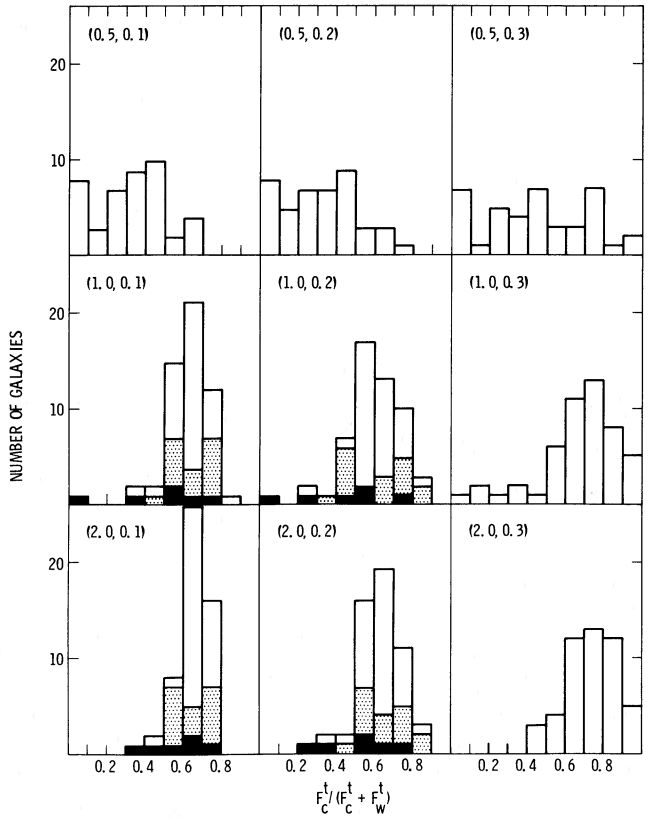

FIG. 7.—Distributions of the fraction of the "total" far-infrared flux arising in the cooler of the two model components. The "total" flux is derived by integration under a modified, single-temperature Planck function. Models are labeled by the values of the flux density ratios of the two-model components, $60/100_w$ and $60/100_c$ (see Table 2 for a conversion to dust temperature). For the four preferred models the latest type galaxies in the sample (Scd-Im) are indicated by the solid areas, and the earliest types (Sab-Sbc) by the hatched areas.

"total" far-infrared flux, and that the intrinsic "total" IRE of the remaining warm OB star-powered emission lies in the range 2–10.

We now assess the nature of these two components further. We would first reemphasize that although this two-component model is successful, it is an oversimplification of reality. In particular some of the large dispersion in Figures 1–6 is likely to be due to (*a*) contributions to the far-infrared flux from sources not dealt with specifically by the model, or (*b*) variations in extinction, IMF, or other parameters.

a) The Cool Component as Cirrus Emission

Emission from dust in the diffuse, neutral medium, heated by the general interstellar radiation field (cirrus-like emission), is the most probable candidate for our cool model component. Low-density H II regions have too low an intrinsic infrared excess (Caux *et al.* 1984), and GMC-embedded young stars produce dust temperatures that are too high (Harvey, Campbell, and Hoffman 1977; Thronson and Harper 1979; Chini *et al.* 1986*a*, *b*; Baud *et al.* 1984).

For the cirrus model to be viable, there must be (*a*) sufficient power in the interstellar radiation field to account for the observed infrared luminosity and (*b*) a large enough optical depth in the diffuse medium to absorb this energy for reradiation in the far-infrared.

Draine and Anderson (1984) have successfully modeled the far-infrared emissivity per H atom of solar neighborhood cirrus clouds by using the interstellar radiation field intensities of Mathis, Mezger, and Panagia (1983), and the grain densities per H atom and physical grain properties of Draine and Lee (1984). In Figure 9 we compare the ratio of the 100 μm flux to the H I line flux of our sample galaxies (Huchtmeier *et al.* 1983) to that predicted by the models of Draine and Anderson (1984, hereafter DA). Figure 9 shows that for many galaxies the cool far-infrared model component of these galaxies can indeed be ascribed to interstellar radiation field heating of the diffuse medium, as modeled by DA, even if the entire medium observed in the 21 cm line is not radiating as strongly as the solar neighborhood cirrus clouds. Some galaxies require somewhat higher than solar radiation fields or dust/H I gas mass ratios for the entire cool component to be attributed to heating by the interstellar radiation field.

The H I flux of galaxies correlates poorly with the 60 and 100 μm emission (Helou 1986*a*) and no improvement is apparent using our cool model component flux. This is not a problem for the model because the H I mass and blue light (and therefore interstellar radiation field) distributions are well known to differ strongly. Our model does explain the apparent existence of an H I mass threshold below which galaxies are

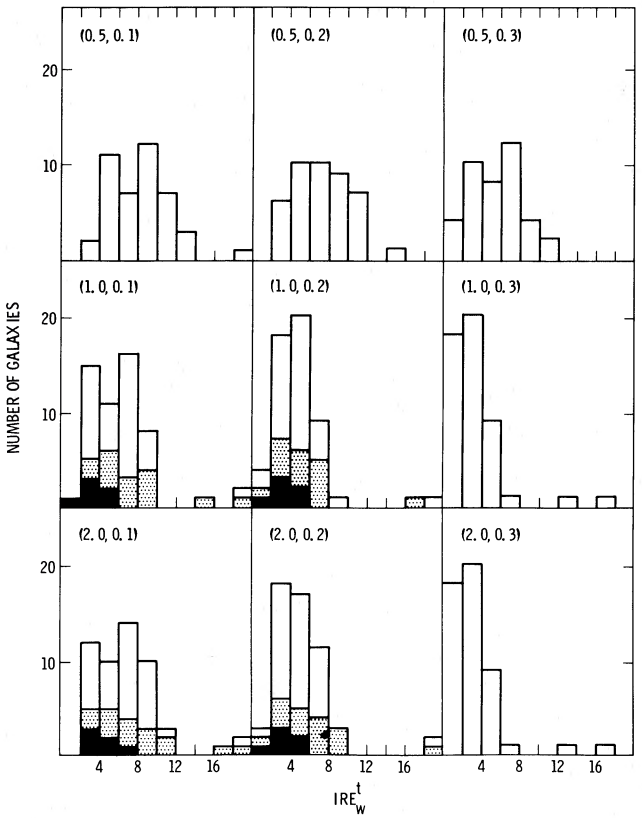

FIG. 8.—Distributions of the "total" infrared excess, IRE_w^t, of the warm model component. IRE_w^t is defined as the "total" (obtained by integration under a modified, single-temperature Planck function) flux of the warm component, divided by the Lyman-alpha flux. Values of IRE_w^t greater than 20 are incorporated into the highest bin. Models are labeled by the values of the flux density ratios of the two-model components, $60/100_w$ and $60/100_c$ (see Table 2 for a conversion to dust temperature). For the four preferred models the latest type galaxies in the sample (Scd-Im) are indicated by the solid areas, and the earliest types (Sab-Sbc) by the hatched areas. For the preferred models, the median IRE_w^t is in the range 4–7.

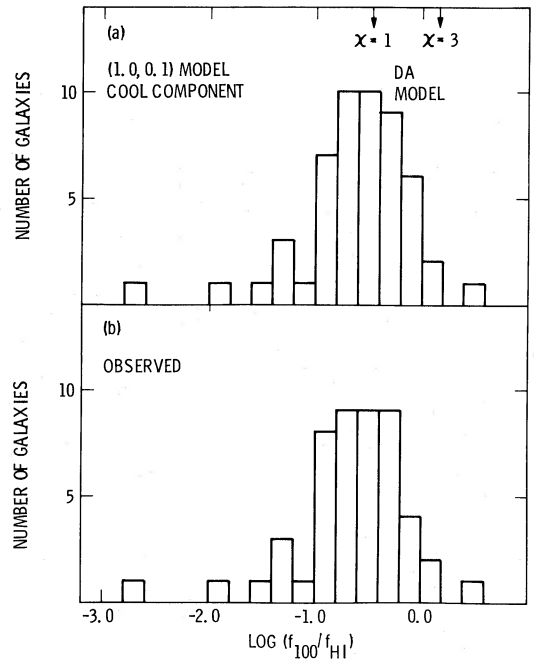

FIG. 9.—Distributions of the ratio of the 100 μm flux to the H I flux ($\times$ km s^{-1}) compared to the predictions of the Draine and Anderson (1984) model at solar and 3 times solar interstellar radiation field intensities. (*a*) for the (1.0, 0.1) model cool component; (*b*) for the entire 100 μm flux. For most galaxies, the DA model is capable of explaining the cool component 100 μm flux.

not detected by *IRAS* (Helou 1986*a*; Bothun 1986), since the cirrus flux will scale with the H I mass. A galaxy model with detailed spatial distributions of H I clouds and the interstellar radiation field, and perhaps also molecular clouds, is needed for a more quantitative evaluation of the cirrus model for galaxy far-infrared emission.

A good test of the existence of the cool component cirrus emission is long-wavelength photometry. For the 15 brightest galaxies at $\lambda > 100$ μm, we tabulate in Table 3 the 250 and 350 μm flux densities expected if (*a*) the 60 and 100 μm emission is interpreted as a single component emitting at the observed temperatures (columns [2] and [3]) and (*b*) the (1.0, 0.1) model is correct (columns [4] and [5]). In the latter case emission from cool dust (18 K for $n = 2$) dominates the 100 μm emission, so the 250 and 350 μm flux densities are 2–5 times higher than if the entire 60 and 100 μm flux is emitted by dust at the observed temperatures (25–32 K for $n = 2$). Very few observations of entire galaxies exist at wavelengths longer than 100 μm, For NGC 4449, observed to have a 150 μm flux density of 100 Jy by Thronson *et al.* (1987) (assuming $n = 1$), our (1.0, 0.1) model ($n = 1$) predicts a 150 μm flux density of 97 Jy, compared to 54 Jy for the single-component model. The success of our model implies that for NGC 4449 a substantial fraction of the 40–120 μm flux is not associated intimately with the OB star complexes. This conclusion is consistent with the result of Thronson *et al.* that the 150 μm flux extends well beyond the Hα image in NGC 4449. Chini *et al.* (1984*a*) have marginally detected NGC 4736 at 1 mm, measuring 4.2 $\pm$ 1.5 Jy. We predict 0.3 Jy for the single-component model of NGC 4736, and 2.3 Jy for the (1.0, 0.1) model. Thus these observations also support the two-component model for the *IRAS* fluxes.

b) *Characteristics of the Warm Component and the Implied Star-Formation Rate*

The mass of dust radiating the warm component (1.0, 0.1) model 100 μm flux ranges from 5×10^3 to 1.5×10^6 $M_\odot$ (see Appendix A for derivation). This is typically 0.1%–0.3% of the dust associated with the entire neutral interstellar medium (where the H I masses have been taken from Huchtmeier *et al.* 1983, and an H I-to-dust mass ratio of 100 has been assumed). The 100 μm emitting dust mass of the (1.0, 0.1) model warm component is also less, by a factor of 1.2 to 4, than the dust mass expected within the ionized regions themselves, assuming no depletion (see Appendix B for an explanation of the calculation of the ionized region dust mass). Thus there is clearly enough dust associated with the diffuse media in the vicinity of the active star-forming regions to radiate the warm component emission. If the far-infrared flux is dominated by very young stars closely related to molecular regions, there is an even larger dust reservoir available.

The infrared excess of our model warm component may be compared with predictions for model H II-regions, which vary from values as low as IRE ~ 3 for low-density H II-regions (Caux *et al.* 1984; Mezger, Mathis, and Panagia 1982) to more than 9 (Hauser *et al.* 1984) depending on assumptions about the IMF and the optical depth of the gas and dust to the ionizing and nonionizing continuum and the lines. Larger values can occur if very young dust-embedded stars dominate the emission or if nonionizing (late B and early A) stars belonging to the OB associations contribute a significant heating flux.

About 10% of the galaxies have $IRE_w^t \sim 2$–3 in the preferred models, including half of the Sd–Im galaxies.

TABLE 3

PREDICTED 250 AND 350 μm FLUX DENSITIES (Jy)

Galaxy	250 μm	350 μm	250 μm	350 μm
	$n = 1$; $n = 2$ (single-component model)		$n = 1$; $n = 2$ (1.0, 0.1 model)	
NGC 278	14.6	7.0	53	33
	8.7	3.2	34	16
NGC 1084.....	19.8	9.6	71	45
	12.0	4.4	45	22
NGC 1087.....	15.7	8.1	48	30
	8.8	3.4	30	15
NGC 1385.....	13.3	6.5	47	30
	8.0	3.0	30	15
NGC 2276.....	12.2	6.1	42	27
	7.4	2.8	27	13
NGC 2976.....	14.2	7.2	46	29
	8.7	3.4	29	14
NGC 3351.....	12.1	5.8	44	27
	7.3	2.7	28	14
NGC 3368.....	13.6	6.9	43	27
	8.3	3.2	28	14
NGC 4027.....	12.6	6.3	42	27
	7.7	3.0	27	13
NGC 4449.....	23.9	11.5	86	54
	14.3	5.3	55	27
NGC 4536.....	11.6	5.4	38	24
	6.8	2.4	24	12
NGC 4654.....	15.6	7.8	53	33
	9.6	3.7	34	17
NGC 4736.....	49.9	24.2	179	113
	30.2	11.1	113	55
NGC 5248.....	17.4	8.5	61	39
	10.6	4.0	39	19
NGC 5676.....	15.1	7.6	48	30
	9.2	3.6	31	15

Unmeasured flux at $\lambda < 40$ μm can only raise IRE_w^t by $\sim 40\%$ at most, and probably much less (see § IIcii and § Vc), so there is little evidence that in these galaxies either (*a*) the integrated Hα emission is seriously affected by extinction, (*b*) substantial trapping by dust of ionizing photons is occurring, or (*c*) GMC-embedded stars or very compact H II regions are a significant fraction of the total OB star population (see also Hunter *et al.* 1986 and Kunth and Sevre 1986). Thus the far-infrared flux of these galaxies comes primarily from the vicinity of the low-density H II regions, and the Hα-derived star-formation rates are probably reasonably accurate.

The observed color temperatures of some of these low-IRE galaxies are high compared to the models for low-density H II regions of de Muizon and Rouan (1985) and Cox, Krugel, and Mezger (1986), which may indicate dominance by relatively high electron density nebulae, excitation by relatively hot stars, or the use of inadequate grain properties by these authors.

For the remainng $\sim 90\%$ of the sample with IRE_w^t in the range 4–10, it is not possible to rule out (*a*) a significant Hα extinction, (*b*) a significant trapping of the ionizing continuum by dust, or (*c*) a contribution to the warm component far-infrared flux from either non-ionizing stars or from very young dust-embedded OB stars. Thus it is possible for these galaxies that star-formation rates derived from Hα fluxes are severely underestimated. This is the case whether Hα is depressed in and around individual H II regions due to extinction or dust trapping, or whether the far-infrared flux is dominated by young OB stars/H II regions in dense and dusty areas.

Derivation of reliable star-formation rates depends on a better understanding of the origin of the far-infrared flux than provided by our simple model, especially in view of the ambiguities in the interpretation of IRE_w^t described above. It is therefore not possible to determine improved star-formation rates for normal galaxies from the far-infrared data at present. Progress toward this end can be made by defining the cool component emission better with $\lambda > 100$ μm photometry, as described in § Va above. Paschen or Brackett line photometry would also be useful to help disentangle the extinction question. Finally, *IRAS* studies of Galactic, and nearby extragalactic, H II regions over the whole H II region luminosity function are also desirable.

c) *Origin of the* $\lambda < 40$ μm *Flux*

Since so few sample galaxies have point-source fluxes of adequate quality at 12 and 25 μm, we have chosen not to address the origin of this emission in detail at this time. A few remarks can be made however. The two-component model is capable of matching the 25 μm fluxes of many galaxies (§ IVb), although that was not an initial constraint. Cirrus emission would seem to be the best candidate for the 12 μm flux (Wynn-Williams and Becklin 1985; Wynn-Williams, Scoville, and Becklin 1985), since cirrus emits strongly at 12 μm in the Galaxy (Gautier 1986), and the observed 100/12 μm flux density ratios of the sample galaxies (0.015–0.06) are similar to those of cirrus (0.02–0.1; Gautier 1986). We have concluded above that cirrus is probably responsible for a good fraction of the 100 μm flux of many galaxies, so 12 μm emission at the general levels observed would be expected on the basis of our models.

VI. SUMMARY AND CONCLUSIONS

The relationship between the integrated Hα flux and the far-infrared flux of spiral disks has been found to have a similar dispersion to that between the far-infrared and the blue flux, suggesting that the far-infrared emission may be as closely linked to the interstellar radiation field from the old disk population as to the very young OB associations. A large spread in the 60/100 μm color temperature and the infrared excess, IRE (the far-infrared flux normalized to the Lyman-alpha flux), has been found, and there is evidence that IRE decreases with increasing 60/100 μm color temperature, with increasing W_λ(Hα) and with bluer UBV colors. This supports the conclusion that nonionizing stars contribute to powering the far-infrared emission.

The far-infrared spiral disk emission can be interpreted in terms of (at least) two thermal components with different temperatures. The low-IRE warm component comes from H II regions, while the high-IRE cool one is interpreted as "cirrus-like" emission (reradiation by dust in the diffuse neutral medium of the interstellar radiation field). These results are similar to those of recent detailed studies of the far-infrared emission of the Galaxy (de Muizon and Rouan 1985; and Cox, Krugel, and Mezger 1986, and references therein). For most of the sample, the cirrus component must be dominated by heating from the old disk population (to explain the correlations with blue flux and $B-V$ color noted above), though the interstellar radiation field of the bluest, highest star-formation rate galaxies may be dominated by a younger population.

For the median spiral, cirrus-like emission contributes 50%–70% of the total far-infrared flux of the galaxy disk. The solar neighborhood cirrus model of DA can account for the majority of the sample. Fluxes at $\lambda > 100$ μm predicted by our model are substantially higher than expected if the 60 and 100 μm fluxes were dominated by emission at the observed color temperature. For two galaxies in our sample with available data, NGC 4449 and NGC 4736 (Thronson *et al.* 1987; Chini *et al.* 1984*a*), the observed flux densities at $\lambda > 120$ μm are in better agreement with the two-component model than with a single-component interpretation.

A small subset of the sample, including half of the Sd and later types, have a low IRE ($< \sim 3$), in general agreement with models for low-density H II regions such as that of Caux *et al.* (1984). These galaxies are unlikely to have any appreciable contribution to the total far-infrared flux from GMC-embedded, optically invisible, young stars. There is little evidence for substantial, previously unsuspected Hα extinction or ionizing photon trapping by dust for these galaxies, so that Hα-derived star-formation rates are not likely to be seriously underestimated.

For the remaining, higher IRE galaxies it is possible that the ionizing stars in optically visible H II regions do not account for all of the flux in the warm far-infrared component, or that extinction of Hα or trapping by dust of ionizing photons is quite important. If one or more of these possibilities is in effect then it is possible that Hα-derived star-formation rates are low by factors of 2–3. This issue cannot be resolved using the far-infrared luminosities because of uncertainties in the IMF, the dust optical depth in and around H II regions, the far-infrared grain emissivity, the possibility of contributions to the heating by late B and early A stars or very young dust-embedded OB stars, and the decomposition of the warm H II region/GMC far-infrared flux from the cool cirrus flux. IREs derived from the same observational quantities for galaxies, Galactic diffuse H II regions, and younger GMC/compact H II region complexes would help in this regard. High-quality Paschen or Brackett line photometry would also help distentangle the Hα extinction question.

The origin of the $\lambda < 40$ μm flux of galaxy disks has not been addressed in any detail here, but it seems quite likely that cirrus emission is responsible for a large fraction of the 12 μm band emission, while the 25 μm band emission can be accounted for by the warm H II regions.

It is a pleasure to thank our colleagues on the *IRAS* project who have made these measurements possible. C. J. P. would like to thank Mount Wilson and Las Campanas Observatories for their generous hospitality and computer resources. We thank W. Rice and G. Bothun for communication of data prior to publication. We also thank G. Bothun, S. E. Persson, C. Beichman, B. T. Soifer, G. Neugebauer, and the referee for critical comments. W. Zhorne was of much assistance in the preparation of the manuscript. The *IRAS* project was managed by the Jet Propulsion Laboratory for NASA. IPAC is supported by NASA.

APPENDIX A

MASS OF DUST RADIATING AT 100 MICRONS

For optically thin emission, the dust mass emitting at a given wavelength is given by

$$M_d = [f_\lambda D^2/B(\lambda, T)]/K(\lambda)\,, \tag{A1}$$

where $K(\lambda) = Q(\lambda)/(4/3)a\rho$ is the mass absorption coefficient, $Q(\lambda) \propto \lambda^{-n}$ is the grain emissivity, a the grain radius, ρ the grain density, and f_λ the flux density at wavelength λ.

Here, we derive the mass of dust in emission at 100 μm. This is, of course, an underestimate of the total dust mass in the galaxy, some of which will be too hot or too cool to radiate at 100 μm.

There are two severe uncertainties associated with the calculation of the 100 μm emitting dust mass. The first is the dust temperature, which is subject to relatively large uncertainties because the 60 and 100 μm bands are close to the peak of the Planck function for these temperatures, and because of the uncertainties in the shape of the *IRAS* 60 and 100 μm transmission curves. The temperature also depends on the adopted value of n. The second uncertainty is the mass absorption coefficient, K. Based on the recent grain model of Draine and Lee (1984), which seems to fit observational data from the UV to the far-infrared very well, we adopt $n = 2$ and K (100 μm) = 90 cm^2 per g. These values are appropriate for Draine and Lee's graphite grains, which dominate the $\lambda > 70$ μm emission in their model. According to Draine and Lee, any larger value for K would violate the Kramers-Kronig relations. If $n = 1$ and $K(100) = 12$ are appropriate (which are more similar to the values adopted by Hildebrand 1983) then the dust masses derived here will *underestimate* the acutal 100 μm emitting dust mass by a factor of about 3.

APPENDIX B

IONIZED GAS MASS AND ASSOCIATED DUST MASS

The total mass of ionized gas in the program galaxies can be derived crudely from the integrated Hα luminosity if assumptions are made as to the density, emission measure, and filling factor. Since the Hα flux is probably dominated by giant diffuse H II regions we have taken an average of these quantities for the giant diffuse H II regions studied by Kennicutt (1984) to derive ionized gas masses. The dust mass associated with the ionized regions was then calculated by using a gas-to-dust mass ratio of 100 (i.e., assuming no depletion).

REFERENCES

Baud, B., *et al.* 1984, *Ap. J.* (*Letters*), **278**, L53.
Becklin, E. E., Fomalont, E. B., and Neugebauer, G. 1973, *Ap. J.* (*Letters*), **181**, 127.
Bothun, G. 1986, private communication.
Burton, W. B., Deul, E. R., Walker, H. J., and Jongeneelen, A. W. 1986, in *Light on Dark Matter*, ed. F. P. Israel (Dordrecht: Reidel), p. 357.
Cataloged Galaxies and Quasars Observed in the IRAS Survey 1985, prepared by C. J. Lonsdale, G. Helou, J. C. Good, and W. Rice (Pasadena: Jet Propulsion Laboratory)
Caux, E., Serra, G., Gispert, R., Puget, J. L., Ryter, C., and Coron, N. 1984, *Astr. Ap.*, **137**, 1.
Chini, R., Kreysa, E., Mezger, P. G., and Gemund, H.-P. 1984*a*, *Astr. Ap.*, **137**, 117.
———. 1986*a*, *Astr. Ap.*, **154**, L8.
———. 1986*b*, *Astr. Ap.*, **157**, L1.
Chini, R., Mezger, P. G., Kreysa, E., and Gemund, H.-P. 1984*b*, *Astr. Ap.*, **135**, L14.
Cox, P., Krugel, E., and Mezger, P. G. 1986, *Astr. Ap.*, **155**, 380.
de Jong, T. 1986, in *Star Formation in Galaxies*, ed. C. J. Persson (Washington D.C.: U.S. Government Printing Office), in press.
de Jong, T., Clegg, P. E., Soifer, B. T., Rowan-Robinson, M., Habing, H. J., Houck, J. R., Aumann, H. H., and Raimond, E. 1984, *Ap. J.* (*Letters*), **278**, L67.
de Muizon, M., and Rouan, D. 1985, *Astr. Ap.*, **143**, 60.
de Vaucouleurs, G., de Vaucouleurs, A., and Corwin, H. 1976, *Second Reference Catalog of Bright Galaxies* (Austin: University of Texas Press) (RC2).
Draine, B. T., and Anderson, N. 1984, *Ap. J.*, **292**, 494. (DA).
Draine, B. T., and Lee, H. M. 1984. *Ap. J.*, **285**, 89.
Drapatz, S. 1979, *Astr. Ap.*, **75**, 26.
Gallagher, J. S., Hunter, D. A., and Tutukov, A. V. 1984, *Ap. J.*, **284**, 556.
Gautier, T. N., III 1986, in *Light on Dark Matter*, ed. F. P. Israel (Dordrecht: Reidel), p. 49.
Harvey, P. M., Campbell, M. F., and Hoffman, W. F. 1977, *Ap. J.*, **211**, 786.
Hauser, M. G., *et al.* 1984, *Ap. J.*, **285**, 74.
Helou, G. 1986*a*, in *Light on Dark Matter*, ed. F. P. Israel (Dordrecht: Reidel, p. 405.
Helou, G. 1986*b*, *Ap. J.* (*Letters*), **311**, Dec. 15.
Hildebrand, R. H. 1983, *Quart. J.R.A.S.*, **24**, 267.
Huchtmeier, W. K., Richter O.-G., Bohnenstengel, H.-D., and Hauschildt, M. 1983, ESO Preprint No. 250.
Hunter, D. A., Gillett, F. C., Gallagher, J. S., Rice, W. L., and Low, F. J. 1986, *Ap. J.*, **303**, 171.
IRAS Explanatory Supplement 1985, ed. C. A. Beichman, G. Neugebauer, H. J. Habing, P. E. Clegg, and T. J. Chester (Washington: Government Printing Office).
IRAS Point Source Catalog 1985 (Washington: Government Printing Office).
IRAS Small Scale Structures Catalog 1986, prepared by G. Helou, and D. Walker (Washington: Government Printing Office).

Kennicutt, R. C. 1983, *Ap. J.*, **272**, 54 (K83).
———. 1984, *Ap. J.*, **287**, 116.
Kennicutt, R. C., and Kent, S. M. 1983, *A.J.*, **88**, 1094 (KK)
Kunth, D., and Sevre, F. 1986, in *Star Forming Dwarf Galaxies and Related Objects*, ed. D. Kunth and T. X. Thuan (Paris: Frontieres), p. 331.
Lequeux, J. 1986, in *Spectral Evolution of Galaxies*, ed. C. Chiosi and A. Renzini (Dordrecht: Reidel), p. 57.
Low F. J., *et al.* 1984, *Ap. J.* (*Letters*), **278**, L19.
Mathis, J. S., Mezger, P. G., and Panagia, N. 1983, *Astr. Ap.*, **128**, 212.
Mezger, P. G. 1978, *Astr. Ap.*, **70**, 565.
Mezger, P. G., Mathis, J. S., and Panagia, N. 1982, *Astr. Ap.*, **105**, 372.
Osterbrock, D. E. 1974, *Astrophysics of Gaseous Nebulae*, (San Francisco: Freeman),
Panagia, N. 1974, *Ap. J.*, **192**, 221.
Perault, M., Boulanger, F., Falgarone, E. and Puget, J. L. 1986, in *Star Formation in Galaxies*, ed. C. J. Lonsdale Persson (Washington: Government Printing Office), in press.
Renzini, A., and Buzzoni, A. 1986, in *Spectral Evolution* of Galaxies, ed. C. Choisi and A. Renzini (Dordrecht: Reidel), p. 195.
Rice, W. L., 1986, private communication.
Rickard, L. J., and Harvey, P. M. 1984, *A.J.*, **89**, 1520.
Rieke, G. H., and Lebofsky, M. J. 1978, *Ap. J.* (*Letters*), **220**, L37.
Rowan-Robinson, M., and Crawford, J. 1986, in *Light on Dark Matter*, ed. F. P. Isreal (Dordrecht: Reidel), p. 421.
Sandage, A., and Tammann, G. 1981, *A Revised Shapley-Ames Catalog of Bright Galaxies* (Washington: Carnegie Institute of Washington) (RSA).
Searle, L., Sargent, W. L. W., and Bagnuolo, W. G. 1973, *Ap. J.*, **179**, 427.
Smith, J. 1982, *Ap. J.*, **261**, 463.
Telesco, C. M., and Harper, D. A. 1980, *Ap. J.*, **235**, 392.
Thronson, H. A., and Harper, D. A. 1979, *Ap. J.*, **230**, 133.
Thronson, H. A., Hunter, D. A., Telesco, C. M., Harper, D. A., and Decher, R. 1987, *Ap. J.*, submitted.
Wynn-Williams, C. G., and Becklin, E. E. 1985, *Ap. J.*, **290**, 108.
Wynn-Williams, C. G., Scoville, N. Z., and Becklin, E. E. 1985, *Ap. J.*, **297**, 607.

GEORGE HELOU and CAROL J. LONSDALE PERSSON: IPAC 100-22, California Institute of Technology, Pasadena, CA 91125